

UNCLASSIFIED

SECURITY CLASSIFICATION OF THIS PAGE (When Data Entered)

REPORT DOCUMENTATION PAGE		READ INSTRUCTIONS BEFORE COMPLETING FORM
1. REPORT NUMBER NSWC TR 83-107	2. GOVT ACCESSION NO. A154 570	3. RECIPIENT'S CATALOG NUMBER
4. TITLE (and Subtitle) A DRAG-AUGMENTED BROUWER-LYDDANE ARTIFICIAL SATELLITE THEORY AND ITS APPLICATION TO LONG-TERM STATION ALERT PREDICTIONS		5. TYPE OF REPORT & PERIOD COVERED Final
7. AUTHOR(s) A. D. Parks		6. PERFORMING ORG. REPORT NUMBER
9. PERFORMING ORGANIZATION NAME AND ADDRESS Naval Surface Weapons Center (K13) Dahlgren, VA 22448		8. CONTRACT OR GRANT NUMBER(s)
11. CONTROLLING OFFICE NAME AND ADDRESS Defense Mapping Agency Washington, DC 20546		10. PROGRAM ELEMENT, PROJECT, TASK AREA & WORK UNIT NUMBERS 35159B
14. MONITORING AGENCY NAME & ADDRESS (if different from Controlling Office)		12. REPORT DATE April 1983
		13. NUMBER OF PAGES 17
		15. SECURITY CLASS. (of this report) UNCLASSIFIED
		15a. DECLASSIFICATION/DOWNGRADING SCHEDULE
16. DISTRIBUTION STATEMENT (of this Report) Approved for public release; distribution unlimited.		
17. DISTRIBUTION STATEMENT (of the abstract entered in Block 20, if different from Report)		
18. SUPPLEMENTARY NOTES		
19. KEY WORDS (Continue on reverse side if necessary and identify by block number) Brouwer-Lyddane artificial satellite theory Atmospheric drag deceleration Satellites; low-altitude earth		
20. ABSTRACT (Continue on reverse side if necessary and identify by block number) —A simple modification is made to the Brouwer-Lyddane artificial satellite theory to account for the effects of atmospheric drag deceleration. The application of this drag-augmented theory to long-term station alert predictions is evaluated for several low-altitude earth satellites.		

DD FORM 1 JAN 73 1473

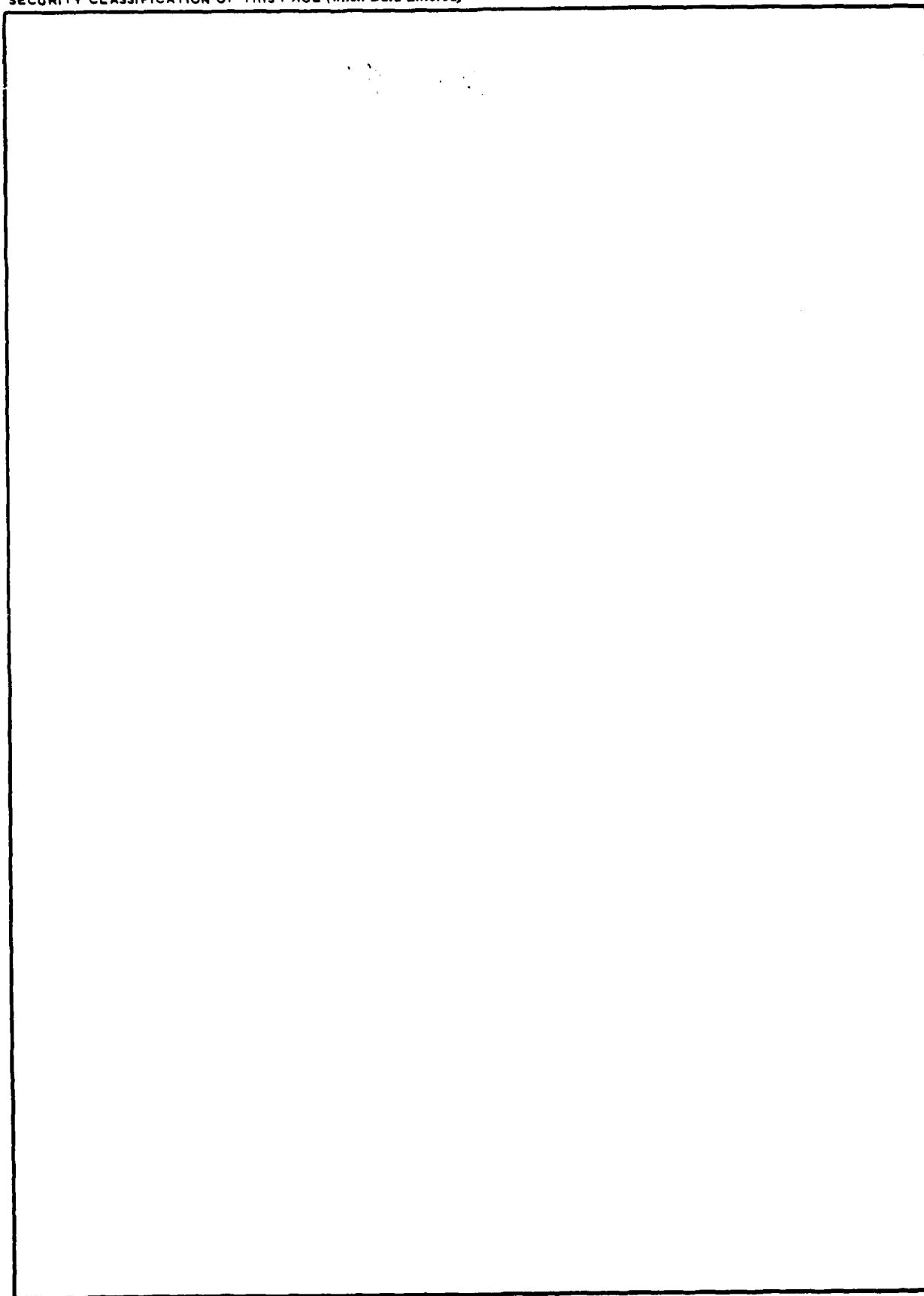
EDITION OF 1 NOV 65 IS OBSOLETE
S/N 0102-LF-014-6601

UNCLASSIFIED

SECURITY CLASSIFICATION OF THIS PAGE (When Data Entered)

UNCLASSIFIED

SECURITY CLASSIFICATION OF THIS PAGE (When Data Entered)



UNCLASSIFIED

SECURITY CLASSIFICATION OF THIS PAGE (When Data Entered)

FOREWORD

This report has been prepared to present a simple modification that can be made to the Brouwer-Lyddane artificial satellite theory to account for the effects of atmospheric drag. This analytic method for generating ephemerides for satellites has been implemented into a station alert prediction algorithm and its accuracy determined for several representative low-altitude earth satellites. The results of this study indicate that significant improvement in predicted satellite ephemerides can be made by introducing this simple drag modification into the Brouwer-Lyddane theory. This document has been reviewed and approved by R. J. Anderle.

Released by:

O. F. Braxton
O. F. BRAXTON, Head
Strategic Systems Department

CONTENTS

	<u>Page</u>
INTRODUCTION.....	1
FORMULATION OF THE DRAG-AUGMENTED BROUWER-LYDDANE METHOD.....	1
EVALUATION METHOD.....	8
RESULTS AND CONCLUSIONS.....	8
DISTRIBUTION.....	(1)

ILLUSTRATIONS

<u>Figure</u>		<u>Page</u>
1	PREDICTION ERROR VS. PREDICTION INTERVAL.....	9

DTIC
ELECTE
S JUN 7 1985 D
B



Accession For	
NTIS GRA&I	<input checked="" type="checkbox"/>
DTIC TAB	<input type="checkbox"/>
Unannounced	<input type="checkbox"/>
Justification	
By	
Distribution/	
Availability Codes	
Dist	Avail and/or Special
A-1	

INTRODUCTION

The Brouwer-Lyddane theory is a general perturbation method that can be used to rapidly predict satellite ephemerides. This theory, however, considers only terrestrial oblateness perturbations in its formulation and takes no account of atmospheric drag accelerations. As a result, the errors induced by the drag-free Brouwer-Lyddane theory into the predicted positions and velocities of low-altitude earth satellites can be quite large and the associated ephemerides unacceptable for scheduling ground station-satellite inview periods. The inability of the Brouwer-Lyddane theory to provide sufficiently accurate long-term tracking schedules for low-altitude satellites can result in undesirable operational difficulties.

This report has been prepared to briefly discuss the effectiveness of a semi-empirical modification that can be made to the Brouwer-Lyddane theory to account for atmospheric drag in a very simple way. This modified theory can be used to predict station alert schedules for low altitude earth satellites with a much more palatable level of accuracy.

A discussion of the formulation of the semi-empirical orbit prediction model mentioned above and a review of the apparent effectiveness of this approach in diminishing drag-induced errors in the predicted satellite rise time that initiate a station inview period are given in the following sections.

FORMULATION OF THE DRAG-AUGMENTED BROUWER-LYDDANE^{1,2} METHOD

The equations given below are those of the drag-augmented Brouwer-Lyddane method and consist of nothing more than the addition of time rates of change terms to the original Brouwer equations for the osculating semi-major axis (a) and eccentricity (e) and for the secular mean anomaly (ℓ). The remaining equations for inclination (i), argument of perigee (g) and right ascension of the ascending node (h) are unchanged. These additive terms in the equations below are enclosed in boxes for easy identification.

¹Brouwer, D., "Solution of the Problem of Artificial Satellite Theory Without Drag," *The Astronomical Journal*, Vol. 64, No. 1274, 1959, pp. 378-397.

²Lyddane, R. H., "Small Eccentricities or Inclinations in the Brouwer Theory of Artificial Satellites," *The Astronomical Journal*, Vol. 68, No. 8, 1963, pp. 555-558.

Prior to the transcription of the drag-augmented equations, the following quantities must be defined:

$$\begin{aligned}
 \dot{a}'' &= \text{semi-major axis decay rate} \\
 \dot{e}'' &= \text{eccentricity decay rate} \\
 \dot{n} &= \text{time rate of change of mean motion} \\
 t &= \text{time from epoch} \\
 n_0 &= (\mu/a''^3)^{1/2} \\
 \eta &= (1 - e''^2)^{1/2} \\
 \theta &= \cos i'' \\
 \gamma_2 &= 1/2 C_{20} a_e^2/a''^2 \\
 \gamma_2' &= \gamma_2 \eta^{-4} \\
 \gamma_3' &= -C_{30} a_e^3 a''^{-3} \eta^{-6} \\
 \gamma_4' &= -3/8 C_{40} a_e^4 a''^{-4} \eta^{-8} \\
 \gamma_5' &= -C_{50} a_e^5 a''^{-5} \eta^{-10} \\
 \alpha &= 1 - 5\theta^2 \\
 \beta &= 1 - 11\theta^2 - 40\theta^4 \alpha^{-1} \\
 \gamma &= 1 - 3\theta^2 - 8\theta^4 \alpha^{-1} \\
 \delta &= 1 - 9\theta^2 - 24\theta^4 \alpha^{-1} \\
 \lambda &= 1 - 5\theta^2 - 16\theta^4 \alpha^{-1} ,
 \end{aligned} \tag{1}$$

where C_{j0} ($j = 2, 3, 4, 5$) are the zonal harmonic gravitational expansion coefficients. Then the secular terms are computed from:

$$\begin{aligned}
 \ell'' &= n_0 t \left\{ 1 + \frac{3}{2} \gamma_2' \eta (3\theta^2 - 1) + \frac{3}{32} \gamma_2'^2 \eta [-15 + 16\eta + 25\eta^2] \right. \\
 &\quad \left. + (30 - 96\eta - 90\eta^2)\theta^2 + (105 + 144\eta + 25\eta^2)\theta^4 \right\} \\
 &\quad + \frac{15}{16} \gamma_4' \eta e''^2 [3 - 30\theta^2 + 35\theta^4] \Big\} + \ell_0'' + \boxed{\dot{n} t^2} \tag{2}
 \end{aligned}$$

$$\begin{aligned}
 g'' &= n_0 t \left\{ -\frac{3}{2} \gamma_2' \alpha + \frac{3}{32} \gamma_2'^2 [-35 + 24\eta + 25\eta^2] \right. \\
 &\quad \left. + (90 - 192\eta - 126\eta^2)\theta^2 + (385 + 360\eta + 45\eta^2)\theta^4 \right\} \\
 &\quad + \frac{5}{16} \gamma_4' [21 - 9\eta^2 + (-270 + 126\eta^2)\theta^2 + (385 - 189\eta^2)\theta^4] \Big\} + g_0'' , \tag{3}
 \end{aligned}$$

and

$$h'' = n_0 t \left\{ -3\gamma_2' \theta + \frac{3}{8} \gamma_2'^2 [(-5 + 12\eta + 9\eta^2)\theta + (-35 - 36\eta - 5\eta^2)\theta^3] \right. \\ \left. + \frac{5}{4} \gamma_4' (5 - 3\eta^2)\theta (3 - 7\theta^2) \right\} + h_0'' \quad (4)$$

The long-period (dependent upon g'') terms are computed from:

$$\delta_1 e = \frac{35}{96} \frac{\gamma_5'}{\gamma_2'} e''^2 \eta^2 \lambda \sin i'' \sin^3 g'' - \frac{1}{12} \frac{e'' \eta^2}{\gamma_2'} (3\gamma_2'^2 \beta - 10\gamma_4' \gamma) \sin^2 g'' \\ - \frac{35}{128} \frac{\gamma_5'}{\gamma_2'} e''^2 \eta^2 \lambda \sin i'' \sin g'' + \frac{1}{4} \frac{\eta^2}{\gamma_2'} \left[\gamma_3' + \frac{5}{16} \gamma_5' (4 + 3e''^2) \delta \right] \\ \sin i'' \sin g'' + \frac{e'' \eta^2}{24\gamma_2'} [3\gamma_2'^2 \beta - 10\gamma_4' \gamma] \quad (5)$$

$$\ell' + g' = g'' + \ell'' + \frac{1}{2} \left\{ \frac{1}{24\gamma_2'} [-3\gamma_2'^2 \{2 + e''^2 - 11(2 + 3e''^2)\theta^2 \right. \\ - 40(2 + 5e''^2)\theta^4 \alpha^{-1} - 400e''^2 \theta^6 \alpha^{-2}\} \\ + 10\gamma_4' \{2 + e''^2 - 3(2 + 3e''^2)\theta^2 - 8(2 + 5e''^2)\theta^4 \alpha^{-1} - 80e''^2 \theta^6 \alpha^{-2}\}] \\ + \frac{\eta^3}{\gamma_2'} \left[\frac{\gamma_2'^2}{4} \beta - \frac{5}{6} \gamma_4' \gamma \right] \left\{ \sin 2g'' + \left\{ \frac{35}{384} \frac{\gamma_5'}{\gamma_2'} \eta^3 e'' \lambda \sin i'' \right. \right. \\ + \frac{35}{1152} \frac{\gamma_5'}{\gamma_2'} \left[\lambda \left\{ -e''(3 + 2e''^2) \sin i'' + \frac{e''^3 \theta^2}{\sin i''} \right\} \right. \\ \left. \left. + 2e''^3 \theta^2 \sin i'' \{5 + 32\theta^2 \alpha^{-1} + 80\theta^4 \alpha^{-2}\} \right\} \cos 3g'' \right. \\ \left. + \left\{ -\frac{\gamma_3 e'' \theta^2}{4\gamma_2' \sin i''} + \frac{5}{64} \frac{\gamma_5'}{\gamma_2'} \left[-e'' \frac{\theta^2}{\sin i''} (4 + 3e''^2) + e''^2 \sin i'' \right. \right. \right.$$

$$\begin{aligned}
& (26 + 9e''^2) \left[\delta - \frac{15}{32} \frac{\gamma_5'}{\gamma_2'} e'' \theta^2 \sin i'' (4 + 3e''^2) \right. \\
& \left. (3 + 16\theta^2 \alpha^{-1} + 40\theta^4 \alpha^{-2}) + 1/4 \frac{\gamma_3'}{\gamma_2'} \sin i'' \right. \\
& \left. \left(\frac{e''}{1 + \eta^3} \right) [3 - e''^2 (3 - e''^2)] + \frac{5}{64} \frac{\gamma_5'}{\gamma_2'} \eta^2 \delta \right. \\
& \left. \left[\frac{e''(-32 + 81e''^4)}{4 + 3e''^2 + \eta(4 + 9e''^2)} \right] \sin i'' \right\} \cos g'' \quad (6)
\end{aligned}$$

and

$$\begin{aligned}
h' = & h'' + \frac{35\gamma_5' e''^3 \theta}{144\gamma_2'} \left\{ \frac{1}{2} \lambda \sin^{-1} i'' + \sin i'' [5 + 32\theta^2 \alpha^{-1} + 80\theta^4 \alpha^{-2}] \right\} \\
& \sin^2 g'' \cos g'' + \frac{e''^2 \theta}{12\gamma_2'} \left\{ -3\gamma_2'^2 [11 + 80\theta^2 \alpha^{-1} + 200\theta^4 \alpha^{-2}] \right. \\
& \left. + 10\gamma_4' [3 + 16\theta^2 \alpha^{-1} + 40\theta^4 \alpha^{-2}] \right\} \sin g'' \cos g'' \\
& + \left\{ -\frac{35\gamma_5'}{576\gamma_2'} e''^3 \theta \left[\frac{1}{2} \lambda \sin^{-1} i'' + \sin i'' (5 + 32\theta^2 \alpha^{-1} + 80\theta^4 \alpha^{-2}) \right] \right. \\
& \left. + \frac{e'' \theta}{4\gamma_2' \sin i''} \left[\gamma_3' + \frac{5}{16} \gamma_5' (4 + 3e''^2) \delta + \frac{15}{8} \gamma_5' (4 + 3e''^2) \right. \right. \\
& \left. \left. (3 + 16\theta^2 \alpha^{-1} + 40\theta^4 \alpha^{-2}) \sin^2 i'' \right] \right\} \cos g'' \quad (7)
\end{aligned}$$

The short periodics (dependent upon E', f', ℓ'') are computed from:

$$\begin{aligned}
a = & \boxed{\dot{a}'' t} + a'' - a'' \frac{\gamma_2}{\eta^3} (3\theta^2 - 1) + \left[\frac{a'' \gamma_2}{(1 - e'' \cos E')^3} \right] \\
& [3\theta^2 - 1 + 3 \sin^2 i'' \cos(2g'' + 2f')] \quad (8)
\end{aligned}$$

$$\begin{aligned}
e = & e'' + \boxed{\dot{e}'' t} + \delta_1 e + \frac{\eta^2 \gamma_2}{2} \left\{ \frac{3\theta^2 - 1}{\eta^6} \left[\frac{e''}{1 + \eta^3} \left\{ 3 - e''^2 (3 - e''^2) \right\} \right. \right. \\
& + \left. \left\{ 3 + e'' \cos f' \cdot (3 + e'' \cos f') \right\} \cos f' \right] + \frac{3(1 - \theta^2)}{\eta^6} \\
& \left. \left[e'' + \left\{ 3 + e'' \cos f' (3 + e'' \cos f') \right\} \cos f' \right] \cos (2f' + 2g'') \right\} \\
& - \frac{\eta^2 \gamma_2'}{2} (1 - \theta^2) [3 \cos (2g'' + f') + \cos (2g'' + 3f')] \quad (9)
\end{aligned}$$

$$\begin{aligned}
i = & i'' - \frac{e'' \theta}{\eta^2 \sin i''} \delta_1 e + e'' \gamma_2' \theta \sin i'' \sin f' \sin (2f' + 2g'') \\
& + 2e'' \gamma_2' \theta \sin i'' \cdot \cos f' \cos (2f' + 2g'') + \frac{3}{2} \gamma_2' \theta \sin i'' \cos (2f' + 2g'') \quad (10)
\end{aligned}$$

$$\begin{aligned}
g + \ell = & g' + \ell' + \frac{\gamma_2'}{4} \left\{ -6\alpha (f' - \ell'' + e'' \sin f') + (3 - 5\theta^2) \right. \\
& \left. [3 \sin (2f' + 2g'') + 3e'' \sin (2g'' + f') + e'' \sin (2g'' + 3f')] \right\} \\
& + \frac{e'' \eta^2 \gamma_2'}{4(1 + \eta)} \left\{ 2(3\theta^2 - 1)(\sigma + 1) \sin f' + 3(1 - \theta^2) \right. \\
& \left. [(1 - \sigma) \sin (2g'' + f') + (\sigma + 1/3) \sin (2g'' + 3f')] \right\} \quad (11)
\end{aligned}$$

$$\begin{aligned}
h = & h' + [2e'' \gamma_2' \theta \cos f' + \frac{3}{2} \gamma_2' \theta] \sin (2g'' + 2f') \\
& - e'' \gamma_2' \theta \sin f' \cos (2f' + 2g'') - 3\gamma_2' \theta (f' - \ell'' + e'' \sin f') \quad (12)
\end{aligned}$$

and

$$e \delta \ell = \frac{1}{2} \frac{e'' \eta^3}{\gamma_2'} \left\{ \frac{1}{4} \gamma_2' \beta - \frac{5}{6} \gamma_4' \gamma \right\} \sin 2g''$$

$$\begin{aligned}
& - \left\{ \frac{1}{4} \frac{\gamma_3'}{\gamma_2'} \eta^3 \sin i'' + \frac{5}{64} \frac{\gamma_5'}{\gamma_2'} \eta^3 \sin i'' (4 + 9e''^2) \delta \right\} \\
& \cos g'' + \frac{35}{384} \frac{\gamma_5'}{\gamma_2'} \eta^3 e''^2 \lambda \sin i'' \cos 3g'' \\
& - \frac{1}{4} \gamma_2' \eta^3 \left\{ 2(3\theta^2 - 1)(\sigma + 1) \sin f' + 3(1 - \theta^2)(1 - \sigma) \sin(2g'' + f') \right. \\
& \left. + \left(\sigma + \frac{1}{3} \right) \sin(2g'' + 3f') \right\}, \tag{13}
\end{aligned}$$

where

$$\sigma = \left(\frac{\eta}{1 - e'' \cos E'} \right)^2 + \left(\frac{1}{1 - e'' \cos E'} \right), \tag{14}$$

the eccentric anomaly E' is obtained from a Newton-Raphson iteration upon the Kepler equation

$$E' - e'' \sin E' = \ell'' , \tag{15}$$

and the true anomaly f' is found from

$$\begin{aligned}
\sin f' &= \frac{\eta \sin E'}{1 - e'' \cos E'} , \\
\cos f' &= \frac{\cos E' - e''}{1 - e'' \cos E'} . \tag{16}
\end{aligned}$$

The final osculating values for a , i , and h are computed from equations (8), (10), and (12), respectively. Equations (2), (9), (11), and (13) are used to calculate final osculating values for ℓ , g , and e from the following relations:

$$A = e \cos \ell'' - e \delta \ell \sin \ell'' , \tag{17}$$

$$B = e \sin \ell'' + e \delta \ell \cos \ell'' , \quad (18)$$

$$\ell = \tan^{-1} (B/A) , \quad (19)$$

$$g = (\ell + g) - \ell , \quad (20)$$

and

$$e = (A^2 + B^2)^{1/2} . \quad (21)$$

All of the input data required to generate the osculating orbital elements from the above-augmented equations; i.e., a'' , \dot{a}'' , e'' , \dot{e}'' , i'' , ℓ_0'' , $\dot{\ell}_0''$, g_0'' , and h_0'' , can be obtained directly from the NAVSPASUR five-card element format data.³ However, the semi-major axis and associated decay rate provided there are the Kaula semi-major axis (a_k) and decay rate (\dot{a}_k) expressed in earth radii. The Kaula semi-major axis can be converted to the desired linear units, when one uses the relation:

$$a'' = a_k a_e \left(\frac{1 + 2X}{1 - X} \right)^{2/3} , \quad (22)$$

where a_e is the earth's semi-major axis,

$$X = \frac{3J_2 (1 - 3/2 \sin^2 i'')}{4 a_k^2 (1 - e''^2)^{3/2}} , \quad (23)$$

and $J_2 =$ zonal harmonic gravitational constant.

Similarly, the desired decay rate \dot{a}'' can be obtained from \dot{a}_k by taking the time derivative of equation (22). This gives

$$\dot{a}'' = \dot{a}_k a_e \left(\frac{1 + 2X}{1 - X} \right)^{2/3} + 2 a_k a_e \dot{X} [(1 + 2X)(1 - X)^5]^{-1/3} , \quad (24)$$

³McCandless, A. R., "NAVSPASUR, SPADATS Type, 5-Card Element Format; description of," memorandum V221:EAT:jmd, 3163, 20 September 1967.

where

$$\dot{X} = X \left[3 \left(\frac{e''}{1 - e''^2} \right) \dot{e}'' - 2 \left(\frac{\dot{a}_k}{a_k} \right) \right]. \quad (25)$$

In the last expression it has been assumed that

$$(\dot{i}'') = 0. \quad (26)$$

EVALUATION METHOD

In order to evaluate the utility of the drag-augmentation method, five-card element sets were obtained from NAVSPASUR for two 92-min. period satellites at 7-day intervals for the timespan from 9 January 1981 through 24 April 1982. During this timespan, these two satellites had perigee altitudes which remained in a 160-nmi to 180-nmi altitude box.

These data were used to generate 30-day predicted station alert schedules every 7 days during the timespan for a single tracking station. The satellite rise times generated near the epochs of the 7-day element sets were assumed to be the true rise times, t_{RT} . These were compared with the associated predicted rise times, t_{RP} , generated for 30 days at 7-day epoch intervals. Orbit adjust schedules, obtained for these two satellites for the span of interest, were used to eliminate those values of t_{RP} which were invalidated due to orbit adjusts occurring at some time during the prediction interval. The remaining valid t_{RP} were differenced with the associated t_{RT} and their absolute values averaged as a function of prediction interval.

RESULTS AND CONCLUSIONS

The results of the averaging procedure described in the previous section are shown in Figure 1 along with the associated 2σ confidence envelope. Also included on this figure is a plot of the errors obtained from a typical drag-free Brouwer-Lyddane prediction for one of the two satellites discussed previously when its perigee altitude was ~ 178 nmi and its argument of perigee was on the sunlit side of the earth. It is apparent from these three curves that the inclusion of the simple drag decay terms in the Brouwer-Lyddane theory has dramatically improved the long-term quality of the predicted satellite rise times.

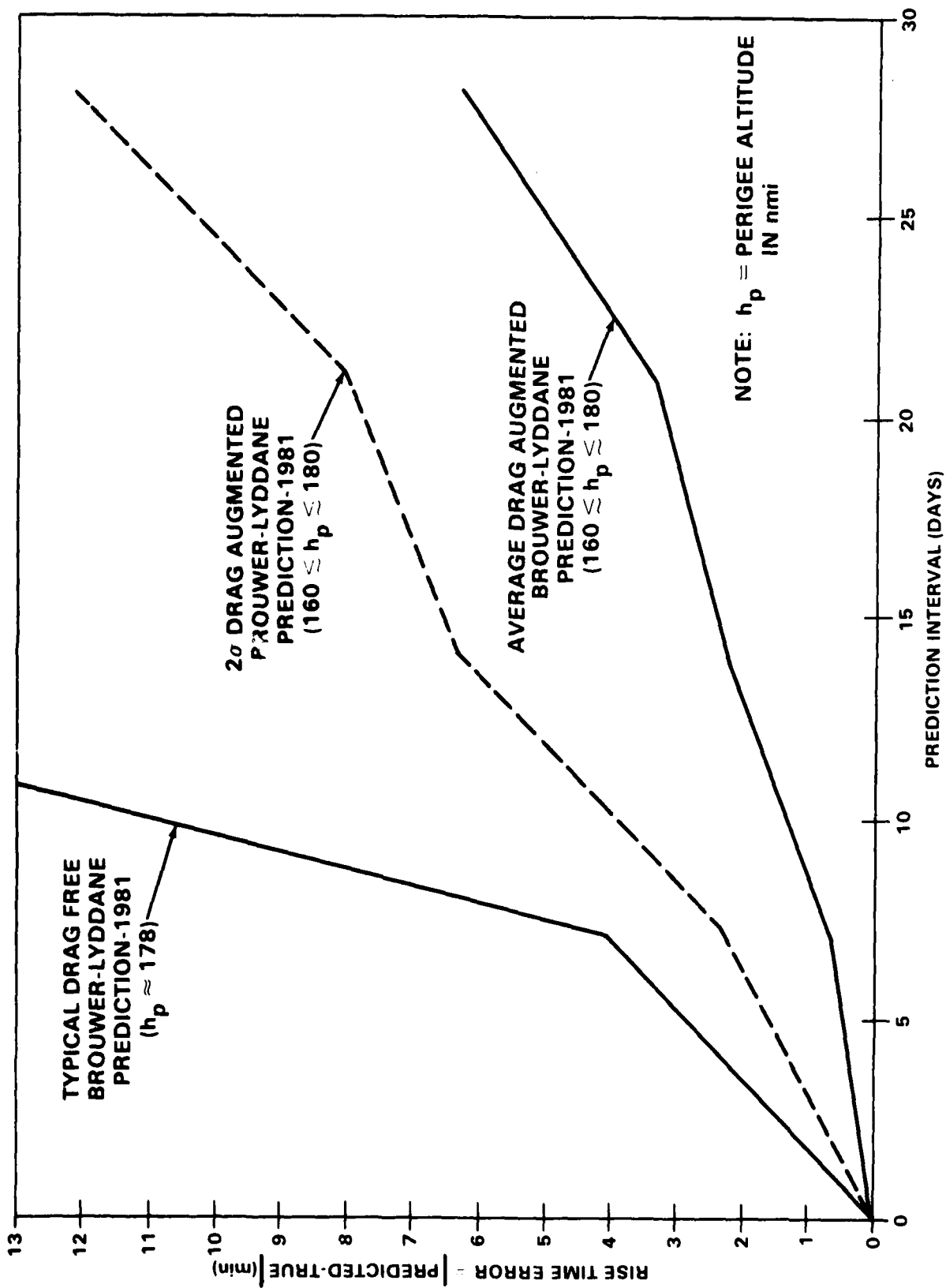


FIGURE 1. PREDICTION ERROR VS. PREDICTION INTERVAL

DISTRIBUTION

Library of Congress Attn: Gift and Exchange Division (4) Washington, DC 20540	Naval Oceanographic Office Bay St. Louis, MS 39522 (2)
National Aeronautics and Space Administration Scientific and Technical Library Code NHS 22, Rm. BA39 600 Independence Avenue, SW Washington, DC 20546 (2)	Office of Naval Research Physical Sciences Division 800 N. Quincy St. (2) Arlington, VA 22217
Defense Mapping Agency Attn: Mr. Jack Calender Washington, DC 20305 (10)	Air Force Geophysics Laboratory Hanscom Field Bedford, MA 01731 (2)
Defense Mapping Agency Hydrographic/Topographic Center Attn: Dr. Patrick Fell (10) Washington, DC 20390	Goddard Space Flight Center Attn: Dr. David Smith (1) Greenbelt, MD 20771
Defense Mapping Agency Aerospace Center Attn: Dr. Robert Ballew (8) St. Louis, MO 63118	The University of Texas at Austin Attn: Dr. Byron Tapley (1) Austin, TX 78712
Naval Electronics Systems Command Navy Space Project, PME106 Washington, DC 20360 (3)	Applied Research Laboratory University of Texas Attn: Dr. Arnold Tucker (5) Austin, TX 78712
Office of Chief of Naval Operations Naval Oceanography Division (NOP-952) Bldg. 1, U. S. Naval Observatory (2) Washington, DC 20350	Physical Sciences Laboratory New Mexico State University Box 3 - PSL Attn: Dan Martin (3) Las Cruces, NM 88003
Naval Research Laboratory Attn: Mr. Al Bartholomew (3) Washington, DC 20375	Applied Physics Laboratory Johns Hopkins University Johns Hopkins Road Attn: Harold Black Laurel, MD 20810 (3)

NSWC TR 83-107

DISTRIBUTION (Continued)

Local:

E31 (GIDEP)

E411

E413 (10)

F14 (4)

K05 (2)

K12 (10)

K13 (30)

K14 (5)